

Acceptor binding energies in GaN and AlN

Francisco Mireles and Sergio E. Ulloa

*Department of Physics and Astronomy, and Condensed Matter and Surface Sciences Program
Ohio University, Athens, Ohio 45701-2979
(Mar 12 1998)*

We employ effective mass theory for degenerate hole-bands to calculate the acceptor binding energies for Be, Mg, Zn, Ca, C and Si substitutional acceptors in GaN and AlN. The calculations are performed through the 6×6 Rashba-Sheka-Pikus and the Luttinger-Kohn matrix Hamiltonians for wurtzite (WZ) and zincblende (ZB) crystal phases, respectively. An analytic representation for the acceptor pseudopotential is used to introduce the specific nature of the impurity atoms. The energy shift due to polaron effects is also considered in this approach. The ionization energy estimates are in very good agreement with those reported experimentally in WZ-GaN. The binding energies for ZB-GaN acceptors are all predicted to be shallower than the corresponding impurities in the WZ phase. The binding energy dependence upon the crystal field splitting in WZ-GaN is analyzed. Ionization levels in AlN are found to have similar ‘shallow’ values to those in GaN, but with some important differences, which depend on the band structure parameterizations, especially the value of crystal field splitting used.

I. INTRODUCTION

Wide-band gap III-V nitrides, particularly Ga-, Al- and InN, and their semiconductor alloys, are materials currently under intense study. Some of their most promising applications in optoelectronics devices are for instance the fabrication of blue/green LED’s,¹ laser diodes,² and ‘solar-blind’ UV photodetectors.³ The performance improvements of these and related optoelectronic devices depend strongly on the features of the intrinsic and extrinsic impurity defects in the nitride compounds. For example, defects and impurities provide free carriers under suitable conditions. Therefore, knowing the accurate position of the donor and acceptor levels of these systems is an issue of great importance in the understanding of optical properties and practical applications of these nitrides.

At present, Mg and Zn are the impurity materials most widely employed in the p-doping of GaN. The experimental thermal ionization energy (acceptor binding energy) associated with Mg is estimated at 250 meV.⁴ The highest doping achieved reaches hole concentrations of approximately $3 \times 10^{18} \text{ cm}^{-3}$ at room temperature.⁵ It is also known that in order to activate the dopants and improve the p-type conductivity, the samples must be

treated with low energy electron beam irradiation, furnace annealing, or rapid thermal annealing after growth.⁶ On the other hand, Zn doping seems to be inefficient because of its relatively deep ionization energy (340 meV).⁴ Other dopants have been considered, but experimental problems like instability and/or hole compensation due to the formation of acceptor-H neutral complexes is still at issue. Estimates for the binding energies of several substitutional acceptors in GaN have been obtained in the past, mostly through photoluminescence (PL) spectra.⁴ However residual impurities and defects in this material complicates the identification of these levels. In contrast, little is known about the doping and spectrum of impurity levels in AlN. In fact, no conclusive results for the doping of AlN with sufficiently high conductivity have yet been reported.

Apart from the question of successful p-doping in GaN and AlN using various impurities, there are still at least two other important issues that are under scrutiny. The first one is related to the determination of the origin of the chemical shift observed in the acceptor spectrum levels in GaN, apparently induced by the differences in the cores of the various impurity atoms, and some possible lattice relaxation around the impurity atom.⁴ The second question is whether acceptors with smaller binding energies (< 230 meV) exist for wurtzite and zincblende GaN. The occurrence of relatively large ionization energies for acceptors in GaN has been attributed in part to the fact that the III-V nitrides are more ionic than other III-V compounds (such as GaAs, GaP and InP), for which the acceptor binding energies are an order of magnitude smaller than those found in GaN. It has also been suggested that the enhanced binding energies found for some acceptors like Zn and Cd, are associated to the relaxation of the d-electron core.⁷ On the other hand, impurities without d-electron states, such as Mg, C, and Si, appear to induce rather shallow acceptor levels. Indeed, very recently, Park and Chadi⁸ examined the stability of acceptor centers in GaN, AlN and BN using first principles calculations. They concluded that the small bondlengths in III-V nitrides inhibit large lattice strain relaxations around impurities (mainly Be, Mg and C), giving rise to relatively shallow states for these species. This would suggest that a similar lack of relaxation accompanies other substitutional impurities in these hosts, producing relatively shallow levels, as long as there are no d-cores close to the valence band energies.

Very recently, the formation energies and impurity levels for a few donor and acceptor species have been studied

theoretically by several groups,^{9–13} employing quantum molecular dynamics schemes and total energy calculations in the local density approximation of density functional theory. In general, consistency is found among those groups, as well as with experimental reports for some impurity levels, such as Mg_{Ga} acceptors (X_Y indicates the ion X substituting in the Y site). However, this is not the case for other acceptors like C_N , where discrepancies of factors of three exist among theoretical values. Although the calculated energy levels for these approaches appear reliable for most cases, the impurity levels reported for some acceptors are close to the systematic error bars introduced in the calculations. The delicate and complex nature of these calculations, which require intensive computations, suggest that alternative methods should be explored in the study of impurity levels in these systems. There is also, no doubt, the need for new careful experiments in the better-characterized materials now available, to clarify these discrepancies. The features of the acceptor states in the different crystal phases, wurtzite (WZ) and zincblende (ZB), have not been discussed either. In order to address these questions, we present here a contribution towards the theoretical treatment of the impurity levels in GaN and AlN based in the effective mass approach for degenerate bands.

In this paper we report effective mass theory calculations of the acceptor binding energies for various impurity atoms in GaN and AlN for both crystal structures, WZ and ZB. Particular attention has been paid to chemical shifts introduced by the foreign atoms. An acceptor-pseudopotential model is used to take into account this effect. The approach used here is based on the effective mass theory (EMT) for degenerate bands. Well parameterized valence band structure calculations are used as input. The results obtained, with no adjustable parameters, are in very good agreement with experiments, as we will see below. Inevitably, the application of even a simple hydrogen-like model of acceptor states in group III-V semiconductors is more complicated than for idealized semiconductors with a single, isotropic and spin-degenerate valence band. The complications are due in part to the band warping and sixfold degeneracy or near-degeneracy of the valence band structure close to the Γ point ($\mathbf{k} = 0$). Since the perturbing potential introduced by the foreign atoms can be seen to zeroth order as pure Coulomb-like, the problem can be seen as a generalized hydrogenic problem, where the kinetic energy of a hole, in the rather complicated valence band structure of the III-V materials, is properly described by a 6×6 matrix Hamiltonian which describes well the dispersion features of the various hole bands. The EMT calculations of the binding energies of Be, Mg, Zn, Ca, and C acceptor impurities are shown to be in very good agreement with the available experiments, and consistent in general with other theoretical calculations employing other methods (with the exceptions discussed above for C, for example). The applicability of EMT for the calculation of impurity

levels with 0.2–0.4 eV binding energies is then verified *post facto*, likely due to the large bandgap in these materials, which yields negligible mixing of conduction band states.

Additionally, we find that the binding energies for acceptors in the ZB structures are predicted to be shallower than their counterparts in the WZ structures, suggesting that doping of ZB material would be of significant practical advantage. We notice that the difference on parameters, mainly the existence of a crystal field splitting for the WZ nitrides, strongly affects the band mixing and correspondingly the binding energies in the two polytypes. It is also likely that differences in the hole masses contribute to the calculated different binding energies. Although substitutional impurities do not represent a strict test of the different band parameterizations, the subtle interplay of the different valence bands on the resulting binding energies provides an interesting overall consistency check of the parameterized band structure.

The paper is organized as follows. In section II, we present the characteristics of the generalized acceptor problem. The explicit matrix form of the ZB and WZ valence band Hamiltonians are also given there. The trial form of the envelope wave functions is presented in section III. The impurity pseudopotential model is discussed in detail in section IV. The correction due to polaron effects is briefly described in section V. The results and discussion are given in section VI, and the conclusions in section VII.

II. GENERALIZED SHALLOW ACCEPTOR PROBLEM

Substitutional impurities with one fewer valence electron than the host atom of the pure crystal introduce well localized acceptor states lying just above the top of the valence band structure. The theory of shallow donor and acceptor states in semiconductors has been reviewed in detail by Pantelides.¹⁴ We assume, as usual, that all acceptor levels in the semiconductor are described within the effective mass theory for degenerate band structures by the following matrix equation

$$\begin{aligned} H(\mathbf{r})\mathbf{F}(\mathbf{r}) &= [\mathcal{H}(\mathbf{r}) + U(\mathbf{r})\mathbf{1}]\mathbf{F}(\mathbf{r}) \\ &= E\mathbf{F}(\mathbf{r}), \end{aligned} \quad (1)$$

where $H(\mathbf{r})$ is the full acceptor Hamiltonian with eigenvalues E for the acceptor states. Here, $\mathcal{H}(\mathbf{r})$ is the Hamiltonian properly constructed from crystal symmetry considerations which entirely describes the spectrum and eigenvalues of a hole near the valence band extremum at the Γ point. Symmetry invariance group theory^{15,16} and $\mathbf{k} \cdot \mathbf{p}$ perturbation theory for degenerate bands^{17,18} has been used to derive the proper effective-mass Hamiltonian for strained semiconductors depending upon the crystal structure.

The potential $U(\mathbf{r})$ is the perturbation produced by the acceptor-ion on the otherwise pure and periodic host crystal. In a simple idealized case, $U(\mathbf{r})$ is taken to be the Coulomb potential $U(\mathbf{r}) = e^2/\epsilon_o|\mathbf{r}|$, where ϵ_o is the static dielectric constant of the crystal, $\epsilon(q = 0, \omega = 0)$, representing a point charge in a dielectric medium. Notice that the screening of the simple hydrogenic potential by a dielectric function $\epsilon(\mathbf{q})$ has been considered in the past as an approach to consider the contribution to the acceptor spectrum of the short range potential from the real impurity.¹⁹ Although this model gives an insight into the specific character of the different atomic acceptor levels, the model results in a generic value for all the impurity defects. This, clearly, neglects the chemical signature of the foreign atoms in the host material (the so-called central-cell contribution).¹⁴ Given these limitations, we employ instead an *ab initio* pseudopotential $U_{ps}(r)$ corresponding to the difference between the bare model potential of the impurity and the host atoms. Since the chemical correction induced by different species is expected to be small and because the pseudopotential used is fairly smooth and without discontinuities, the effective mass approach is expected to yield an appropriate description of the system. More details on the impurity potentials used are given in section IV.

In Eq. (1), $\mathbf{1}$ is the 6×6 unit matrix and $\mathbf{F}(\mathbf{r})$ is a column vector whose $F_j(\mathbf{r})$ elements characterize the envelope function which modulates the Bloch functions $\phi_j(\mathbf{r})$ of the unperturbed crystal at the top ($\mathbf{k} \approx 0$) of the valence structure. Correspondingly, the wave functions for the shallow states are given by

$$\psi(\mathbf{r}) = \sum_{j=1}^6 F_j(\mathbf{r}) \phi_j(\mathbf{r}). \quad (2)$$

The trial form chosen for the envelope functions $F_j(\mathbf{r})$ is discussed in detail in section III. In the following subsections we describe briefly the explicit form of the hole Hamiltonian $\mathcal{H}(\mathbf{r})$ for the two crystal polytypes (WZ and ZB), in which the bulk GaN and AlN semiconductors grow.

A. Wurtzite valence band Hamiltonian

In order to consider the motion of a carrier at the top of the valence band in a wurtzite semiconductor we must take into account its six-fold rotational symmetry, which induces a crystal field splitting. Moreover, in the case of spin-orbit interaction, the Γ_{15} level splits into the Γ_9 state, upper Γ_7 level, and lower Γ_7 level, corresponding to the heavy hole, light hole and split-off hole bands.¹⁵ The appropriate effective mass Hamiltonian that reflects those features of the WZ GaN bulk crystal should be described thus by the Rashba-Sheka-Pikus Hamiltonian (RSP),^{15,16} as discussed recently by Sirenko *et al.*²⁰ In the vicinity of the valence band maximum, and to second

order in k , the six states (including the spin index) of the RSP Hamiltonian for unstrained WZ structures can be explicitly written in a matrix representation as follows:

$$\mathcal{H}_{WZ}(\mathbf{k}) = \begin{pmatrix} F & 0 & -H^* & 0 & K^* & 0 \\ 0 & G & \Delta & -H^* & 0 & K^* \\ -H & \Delta & \lambda & 0 & I^* & 0 \\ 0 & -H & 0 & \lambda & \Delta & I^* \\ K & 0 & I & \Delta & G & 0 \\ 0 & K & 0 & I & 0 & F \end{pmatrix}, \quad (3)$$

where

$$\begin{aligned} F &= \lambda + \theta + \Delta_1 + \Delta_2 \\ G &= \lambda + \theta + \Delta_1 - \Delta_2 \\ \lambda &= A_1 k_z^2 + A_2 k_{\perp}^2 \\ \theta &= A_3 k_z^2 + A_4 k_{\perp}^2 \\ H &= i(A_6 k_z k_{\perp} + A_7 k_{\perp}) \\ I &= i(A_6 k_z k_{\perp} - A_7 k_{\perp}) \\ K &= A_5 k_{\perp}^2 \\ \Delta &= \sqrt{2} \Delta_3, \end{aligned} \quad (4)$$

with $k_{\perp}^2 = k_x^2 + k_y^2$, and $k_{\pm} = k_x \pm i k_y$. Here, Δ_1 corresponds to the energy splitting produced by the anisotropy of the hexagonal symmetry, $\Delta_2 = \Delta_{so}^{(z)}/3$ and $\Delta_3 = \Delta_{so}^{(\perp)}/3$ are the energy splittings for the z and perpendicular directions produced by the spin-orbit (SO) interaction.²⁰ The A constants are related to the inverse of the hole masses, in units of $\hbar^2/2m_o$, where m_o is the bare electron mass. Notice that when the linear terms in (3) are negligible ($A_7 = 0$; which is in fact nearly the case in GaN and AlN), the RSP Hamiltonian has complete inversion symmetry. This symmetry allows for helpful simplifications in dealing with the acceptor problem in the envelope function framework, as we discuss below.

B. Zincblende valence band Hamiltonian

In the case of semiconductors with the ZB structure, the hole wave functions characterizing the sixfold degenerate Γ_{15} state split, due to the effects of spin-orbit interaction, into the fourfold degenerate Γ_8 states corresponding to the heavy and light hole bands, and the spin-split off hole states Γ_7 .¹⁵ The Hamiltonian which takes into account all these features of the cubic symmetry for ZB semiconductors is the well known Luttinger-Kohn Hamiltonian (LK),¹⁷ which at the valence band extremum, and to second order in k , is expressed in terms of only four empirical parameters — the so-called Luttinger-Kohn parameters γ_1, γ_2 and γ_3 , and the spin-orbit splitting Δ_o . Thus, the LK Hamiltonian \mathcal{H}_{ZB} is written in matrix form as follows

$$\mathcal{H}_{ZB}(\mathbf{k}) = \begin{pmatrix} P & L & M & 0 & N & S \\ L^* & Y & 0 & M & R & \sqrt{3}N \\ M^* & 0 & Y & -L & \sqrt{3}N^* & R \\ 0 & M^* & -L^* & P & -S^* & N^* \\ N^* & R^* & \sqrt{3}N & -S & W & 0 \\ S^* & \sqrt{3}N^* & R^* & N & 0 & W \end{pmatrix}, \quad (5)$$

where

$$\begin{aligned} L &= -2\sqrt{3}i\gamma_2 k_z k_- \\ M &= \sqrt{3}\gamma_3(k_x^2 - k_y^2) - 2\sqrt{3}i\gamma_3 k_x k_y \\ N &= \frac{i}{\sqrt{2}}L \\ P &= \gamma_1 k^2 - \gamma_2 (2k_z^2 - k_\perp^2) \\ Q &= \gamma_1 k^2 + \gamma_2 (2k_z^2 - k_\perp^2) \\ R &= -\frac{\sqrt{2}}{3}i(P - Q) \\ S &= -i\sqrt{2}M \\ W &= \frac{1}{3}(2P + Q) + \Delta_o \\ Y &= \frac{1}{3}(P + 2Q). \end{aligned} \quad (6)$$

Here, L, M, P and Q are in units of $\hbar^2/2m_o$. Notice that the higher symmetry of the ZB structure produces a much simpler $\mathcal{H}(r)$ and fewer parameters than for the RSP case. In both cases, the operator $\mathcal{H}(\mathbf{r})$ is obtained via the usual transformation $k_\alpha \rightarrow i\frac{\partial}{\partial x_\alpha}$ in $\mathcal{H}(\mathbf{k})$.

III. TRIAL FORM FOR THE ENVELOPE FUNCTIONS

To solve the effective mass equation for degenerate bands, Eq. (1), we use the fact that the effective mass Hamiltonian is invariant under inversion with respect to the origin, so that the envelope functions $F_j(\mathbf{r})$ can be chosen to have definite parity. Since the features of the acceptor problem are rather like those of a hydrogenic-like problem, it has proved convenient to choose the envelope functions basically as an expansion in spherical harmonics and a linear combination of hydrogenic-like radial functions. In particular, we have chosen the following explicit form:

$$F_j(\mathbf{r}) = \sum_{l,m} f_l^j(r) Y_{lm}(\theta, \phi), \quad (7)$$

summing over all l even (or odd), and with radial functions for a given hole band j and angular momentum quantum number l of the form

$$f_l^j(r) = \sum_{i=1}^N A_i^j r^l e^{-\alpha_i r}. \quad (8)$$

In this work, however, we are mostly interested on the ground state (the highest binding acceptor state), and in such state only even l will contribute to the expansion — as one would expect a ground state with even parity. This convenient simplification can be relaxed straightforwardly if desired, with little effect on the results. For numerical convenience, we find it useful to minimize or evaluate the acceptor binding energy choosing α_i 's in the progression $\alpha_k = \alpha_1 e^{\beta(k-1)}$, such that $\beta = (N-1)^{-1} \log(\alpha_N/\alpha_1)$, and the end point conditions are chosen as $\alpha_1 = 1.2 \times 10^{-2} a_o^{*-1}$, and $\alpha_N = 3.5 \times 10^2 a_o^{*-1}$. Here, $a_o^* = \tilde{\gamma}_1 \epsilon_o a_o$ is the effective Bohr radius, and $\tilde{\gamma}_1$ is defined by

$$\tilde{\gamma}_1 = \begin{cases} -(2m_o/\hbar^2)(A_2 + A_4) & \text{for WZ} \\ \gamma_1 & \text{for ZB} \end{cases}, \quad (9)$$

such that the effective Rydberg energy is defined as $E_o^* = m_o e^4 / 2\hbar^2 \tilde{\gamma}_1 \epsilon_o^2 = e^2 / 2a_o \tilde{\gamma}_1 \epsilon_o$. The range of α_i values was designed to cover a wide spectrum of length scales. In the limit case of $\tilde{\gamma}_1 = \epsilon_o = 1$ (with $N=25$ and for $l = 0, 2$), one obtains the hydrogen spectrum, so that for the first five states we obtain (in Rydbergs) $E_1 = 1.0000$, $E_2 = 0.2500$, $E_3 = 0.1111$, $E_4 = 0.0625$ and $E_5 = 0.0399$, as expected.

IV. IMPURITY ATOM PSEUDOPOTENTIAL

As mentioned above, a simple hydrogenic (scaled Coulomb) potential would not yield the observed variations in the binding energy of acceptor states for different impurity atom species. Photoluminescence measurements show indeed important differences in the acceptor binding energies in WZ GaN for different impurities⁴. To study those ‘chemical’ shifts one needs to use impurity potentials properly constructed to insure that their physical properties reflect the expected shifts. The impurity potential here is obtained from an analytical representation of the pseudopotential for the bare impurity and host atoms. The analytic form follows Lam *et al.*,²¹ who fit the first-principles pseudopotentials developed earlier by Zunger *et al.*²² in a density functional formalism. Notice then that the acceptor potential is truly an impurity pseudopotential, having its origin in *ab initio* calculations. The pseudopotential for a bare atom can be written as²¹

$$U_{ps}(r) = \sum_l V_{ps}^l(r) \hat{P}_l - \frac{Z_v}{r}, \quad (10)$$

with

$$V_{ps}^l(r) = \frac{C_1^l}{r^2} e^{-C_2^l r} - \frac{Z_c}{r} e^{-C_3 r}, \quad (11)$$

where $V_{ps}^l(r)$ represents the atomic core pseudopotential. \hat{P}_l is the projection operator which picks out the compo-

ment of the wave function with angular momentum number l . The constants C_1^l , C_2^l and C_3 are the fitted parameters, with Z_c and Z_v representing the core and valence electron charges, respectively, as defined by Lam.²¹ The first term in (11) represents a potential barrier which replaces the kinetic energy of the true valence states, while the second term arises from electrostatic screening of the nucleus by the core electrons and exchange-correlation forces. Using these pseudopotentials, the impurity model potential is constructed as follows.

When the substitutional impurity atom replaces the host atom in the crystal, the impurity potential is defined as the difference between the impurity and host ion pseudopotentials. If $l = 0$, for instance,

$$U(r) = \frac{e^2}{\epsilon_o} \Delta V_{ps}^o(r) - \frac{\Delta Z_v e^2}{\epsilon_o r}, \quad (12)$$

with

$$\Delta V_{ps}^o(r) = \pm(V_{ps,host}^o(r) - V_{ps,imp}^o(r)) \text{ for } Z_{host} \gtrsim Z_{imp}. \quad (13)$$

Here, $\Delta Z_v = Z_v^{host} - Z_v^{imp}$ ($= 1$ for single acceptors), and ϵ_o is the dielectric constant of the host lattice. Clearly the first term in $U(r)$ corresponds to the net potential produced by the difference between the bare core potentials of the impurity and the host; it is the short-range part. The last term is the long-range Coulombic potential due to the difference in the valence charge ΔZ_v . The static dielectric constant ϵ_o is introduced here to reflect the effect of the lattice polarizability (screening) of the host crystal. Notice that in this approach the net effect of the redistribution of charge near the impurity defect and the accompanying screening of the foreign charge at 'large' distances (several lattice units) is considered fully in the pseudopotential definition.

In a different approach, frequent in the literature,²⁹ the role of the pseudopotential is partly simulated using a q -dependent screening function $\epsilon(q)$ ($\rightarrow \epsilon_o$ for $q \rightarrow 0$) in the simple hydrogenic-style impurity potential. We avoid using $\epsilon(q)$ thanks to the impurity-specific pseudopotential. We believe our approach to be better in this problem, as it requires no further adjustable parameters and yields the expected chemical shifts quite accurately.

To provide a simple and independent test of the model we have calculated the binding energies for several acceptors in the well characterized semiconductor GaAs. The results are shown in Table I. The theoretical binding energies are in excellent agreement with the experimental values, with no additional parameters.

V. POLARON CORRECTION

We should also notice that since the nitride semiconductors (GaN and AlN) are polar materials, one would expect that the electron-LO phonon coupling would introduce corrections to the bound states. In order to

obtain an estimate of such correction, we assume that the polaron contribution to the acceptor binding energy close to the Γ point is diagonal in band index. Therefore the acceptor binding energies will be enhanced by $(1 + \alpha_F(m_j^*)/6)E_{o,j}^*$, up to first order in the Fröhlich coupling constant α_F for each hole band. This coupling constant is defined by²³

$$\alpha_F(m_j^*) = \left(\frac{1}{\epsilon_\infty} - \frac{1}{\epsilon_o} \right) \left(\frac{E_o}{\hbar\omega} \frac{m_j^*}{m_o} \right)^{1/2}, \quad (14)$$

where E_o is one Rydberg, $E_{o,j}^*$ is the ground state energy of the impurity acceptor without the polaron correction, $\hbar\omega$ is the LO phonon energy, and m_j^* is the average j -hole effective mass. In this way, the contribution of each hole band to the polaron energy is taken into account explicitly in the multiband calculation. Let us notice that the resulting polaron correction is relatively small (not greater than 8%) in all cases, as shown in the tables below, despite the polar nature of these materials. This is presumably due to the fact that the coupling constant associated to each hole band is relatively small (≤ 1.5) in all cases.²⁴

VI. RESULTS AND DISCUSSION

Since the reported values of effective mass parameters obtained by different approaches for both the RSP and LK Hamiltonians may have significant discrepancies, we have used different sets of parameterizations in order to compare the resulting impurity states.^{25–30}

For the wurtzite system (Tables II and III), we use Kim *et al.*²⁵ RSP parameterizations obtained by full potential linearized muffin-tin orbital (FP-LMTO) band structure calculations, in which the spin-orbit coupling effects were obtained via the atomic-sphere approximation. We have also used the Suzuki *et al.*²⁶ RSP parameters obtained by full potential linearized augmented plane wave calculations (FLAPW); a different set reported by Majewski *et al.*²⁷ based on the norm-conserving pseudopotential plane-wave (PPPW) method, and a fourth set obtained by Yeo *et al.*,²⁸ who employ an empirical pseudopotential method. Notice that differences in parameters between these two groups are typically small, but can be substantial in some cases (such as the value of the crystal field splitting Δ_1), having important consequences on the binding energy calculations, as we see later.

In the case of zincblende structures, the LK hole-parameters used are those reported by Kim *et al.*,²⁵ and Suzuki *et al.*²⁶ as mentioned above, and a third set by Wang *et al.*,²⁹ based on pseudopotential calculations. These parameters are summarized in Table IV.

We first examine our results for the acceptor levels in WZ nitrides. We should emphasize here that the experimental values of the acceptor levels in WZ-GaN are not without controversy. Nevertheless, in order to have a trend of the binding energies for different dopants, we

compare our theoretical calculations with the experimental values in the literature. For GaN the results are listed in Table V (theoretical binding energy values are reported here to the nearest meV, but are calculated with much higher numerical accuracy for each set of parameters). We note that in general the binding energies for different impurities are in good agreement with those values observed in experiments. For instance, our calculations with the Suzuki *et al.*²⁶ parameters give rise to a binding energy for Be_{Ga} and Mg_{Ga} (241 and 253 meV, respectively, with the polaron correction included) which would seem to be in better accord with the reported experimental value (250 meV). Indeed, Salvador *et al.*³¹ reported recently room-temperature photoluminescence spectra of Be-doped GaN films. They found strong features in the 390-420 nm range which were attributed to the acceptor state formed by Be at about 250 meV above the valence band edge. Even though residual impurities could be responsible as well for this level, no experiments have been reported to confirm either claim. Very recently, Bernardini *et al.*¹⁰ using first principles calculations, predict that Be is a shallow acceptor in GaN with a binding energy (BE) of only 60 meV, in clear contrast with our calculations and with the experimental data. It is interesting to note, however, that our BE's for Mg (~ 200 -250 meV) are in satisfactory agreement with those theoretical values obtained from first principles calculations by Fiorentini *et al.*¹² (~ 230 meV) and Neugebauer *et al.*¹¹ (~ 200 meV).

In contrast, the binding energies with Ref. [26] parameters, for Zn and C impurities, are overestimated with respect to the experimental values (presumably due to the high value of crystal field reported in [26]). In principle we should expect the best fit precisely for these impurities since they are isocoric with Ga and N, respectively, which would produce negligible local relaxations and core polarization effects. The best agreement occurs when we use the parameters from Kim *et al.*,²⁵ suggesting that their parameter set is somewhat better. For example, for Zn_{Ga} in GaN, we obtain a BE of 331 meV using Kim's parameters, which is in good agreement with the experimental value of 340 meV, and in excellent agreement with the theoretical value reported by Bernardini *et al.* (330 meV).¹³ Concerning the C_N substitutional impurity in a N site, we find that with exception of Suzuki's parameters, all the hole-band sets give BE's (223-240 meV) comparable with the experimental value of 230 meV from Fischer *et al.*³² Note that using Kim's parameters gives the acceptor level just even with the experimental value, in a nice but probably fortuitous agreement, considering the possible sources of systematic errors. Boguslawski *et al.*⁹ had predicted also an ionization energy for C_N of ~ 200 meV, while Fiorentini *et al.*¹² report a deeper (~ 600 meV) value. The formation energy for this impurity is found to have also a substantial difference (1.4 eV) between those authors. The relatively higher relaxation effects predicted by Ref. [9] seem to play a more crucial role here. Similar discrepancies are found between

the present work and other calculations for Ca_{Ga} and Si_N .⁹ We found that Ca_{Ga} has its acceptor level (~ 260 meV), close to that of the Mg. It is interesting to notice that temperature-dependent Hall measurements of Ca-doped GaN have shown that the thermal ionization energy level of Ca (~ 0.17 eV) is similar to that found in Mg (~ 0.16 eV).^{37,38} This could indicate that the acceptor binding energy for Ca is also close to that for Mg as we have indeed predicted. Similarly, Si_N was found to have a rather shallow level in WZ-GaN at about 0.2 eV. While the donor behavior of Si is well known, no reliable experimental evidence of Si acceptor has been reported.

The collection of results discussed above indicates that the parameterization of Kim *et al.*²⁵ leads to acceptor binding energies in overall better agreement with the experiments and other theoretical estimates. Notice however that the differences in binding energies in GaN with other sets of parameters are not large in most cases, within a few percent from each other.

We would like now to comment on the effect of the crystal field splitting on our calculations. Whereas recent experiments seems to indicate that the Δ_1 value is about 10 meV,³³⁻³⁵ the theoretical estimates are still controversial, varying between 22-73 meV for GaN depending upon the approach used.²⁵⁻²⁸ For example, Ref. [25] and [26] had obtained $\Delta_1 = 36$, and 73 meV, respectively. The former authors attribute the large theoretical discrepancy to the use of an ideal-cell internal structure parameter u in Ref. [26], instead of the relaxed one. In any case, to illustrate the effect of the binding energies upon the Δ_1 value, we show in Fig. 1 their dependence on this parameter for Mg_{Ga} in WZ-GaN, over a wide range. A rather monotonic behavior is seen in the binding energies, as one would expect. Note that for all parameter sets (with exception of those in Ref. [27]) the BE's are consistently close for each Δ_1 value. Note that using the experimental value of 10 meV for Δ_1 would produce smaller binding energies, giving values of about 0.19 eV, regardless of the set employed. The behavior for other dopants shows an analogous trend, where the energy shift on the binding energy is nearly the difference in Δ_1 values. This discussion indicates that additional experimental evidence for a smaller Δ_1 value, and comparison with better optimized estimates, would be of interest.

The results for AlN in the wurtzite structure are given in Table VI. The first thing to notice here is that due perhaps to the large discrepancy in Δ_1 values, -215, -219, and -58 meV for Kim,²⁵ Majewski,²⁷ and Suzuki,²⁶ respectively, the binding energies differ by almost a factor of two for different parameter sets. Notice further that values of A_5 and A_6 also differ substantially for different authors, strongly affecting the band mixing and corresponding binding energies. Given the better agreement of Kim *et al.* parameters in WZ-GaN, we are inclined to think that the corresponding results in WZ-AlN will be perhaps closer to the experimental results. Unfortunately, as we mentioned earlier, the experimental spectrum for acceptors in AlN is unknown at present (due

to the well known difficulties in doping this material⁴). Further scrutiny of the parameters reported by these and future authors should be carried out to solve the disagreements. Notice that the BE of C_N in WZ-AlN is found to exceed 0.65 eV in our calculations for all three sets of parameters (not shown in Table VI). This value, in the limit of validity perhaps of our EMT calculations, suggests nevertheless that such impurity will yield a somewhat deeper level than those reported in Table VI. Although substitutional impurity calculations do not represent a strict test of the band parameterizations, the subtle interplay of the different valence bands on the resulting binding energies (or even excited impurity states) provide an interesting overall consistency check.

For the ZB phase, we notice that predicted binding energies are consistently smaller (by nearly a factor of two) than in the WZ structure of GaN. Indeed, typical differences of roughly 100 meV are found in the binding energies between the two phases (ZB and WZ) in this material. This would have important consequences in electronic uses once doping of ZB phases is stabilized. Concerning the resulting impurity binding energies for GaN, we observe that the LK parameters given by Ref. [25], [26], and [29] give rise to binding energies which are in close agreement with each other. We should also comment that a different set of band parameters in the ZB phase has been given by Meney *et al.*, using a semi-empirical perturbative approach.³⁰ However, using these parameters result in BE's much smaller than those presented here. This difference, even greater in the binding energies for ZB-AlN, reflects the more approximate nature of the parameters in Ref. [30]. Notice that the Luttinger γ -parameters in Kim *et al.* are slightly smaller than for Suzuki *et al.* (or equivalently, slightly larger effective masses), which would be expected to yield slightly larger BE's for the former set of parameters, as is clearly seen in Table VII.

Recent PL spectra of cubic GaN by As *et al.*³⁹ had claimed as indeed we have predicted in our calculations, that acceptor BE's for cubic-GaN may have energies shallower than these in wurtzite-GaN. Acceptor energies of about 130 meV have been estimated by them. This in very good agreement with our calculations; as we can see in Table VII, the BE's ranges from ~ 130 meV for Si to ~ 180 meV for Zn. This acceptor level has not been identified and it is probably produced by residual impurities.

The smaller binding energies in ZB, with respect to impurities in the WZ structure, is an interesting result that should be understood in terms of the different band structure parameters. Notice, however, that the difference in the effective Rydberg energy for WZ and ZB GaN, is not large at all, as seen in Tables II and IV. Similarly, the effective Bohr radius for both structures is nearly the same, as illustrated in the fact that $\tilde{\gamma}_1$ is of the same order in both cases, and that the dielectric constant for both polytypes has been taken as $\epsilon_o = 9.5$. The polaron correction is certainly relatively small also, and is therefore not a

possible source of the binding energy difference in these polytypes. However, the parameter that apparently gives rise to these large shifts in the acceptor energies could be identified with the in-plane heavy hole mass, which is indeed larger in wurtzite than in zincblende for both GaN and AlN, and hence produces larger binding energies. In order to verify the effect of the different effective masses in the two polytypes, we have calculated the acceptor levels for WZ-GaN using the quasicubic sets of parameters of Ref. [25], with the same crystal field splitting than the obtained for the non-quasicubic set. It turns out that the binding energies are smaller correspondingly, which confirms our assumption. One should also mention that just as seen in Fig. 1, a vanishingly small Δ_1 (as is the case in ZB) would produce an even smaller binding energy for a given impurity. [This would also explain the agreement among the three sets of parameters, since Δ_1 differences are the most significant for different authors.] We then conclude that it is in fact a combination of the crystal field splitting and slightly larger hole masses that produce larger binding energies in WZ than in the ZB structure. An interesting and important effect of the different lattice and band structure.

VII. CONCLUSION

We have carried out calculations for the shallow acceptor energies associated to different substitutional impurity atoms in GaN and AlN hosts. The calculations were performed within the effective mass theory, taking into consideration the appropriate valence band Hamiltonian symmetries for the WZ and ZB polytypes, and using the full 6×6 acceptor Hamiltonian and included the actual spin-orbit energy splitting. In addition, the impurity pseudopotential and the electron-phonon (polaron) correction has been explicitly considered. These more realistic treatment allows us to compare directly with the observed data and verify that our calculation produces the appropriate 'chemical shifts'. Indeed, our calculations of the acceptor binding energies are in quite good agreement with PL experiments, as the introduction of the impurity pseudopotential seems to be an excellent model to describe the chemical shifts associated with each impurity atom. It is interesting that the good fits were found without any adjustable parameters in the calculation, once the contribution due to the electron-phonon polar interaction was included. We find that small differences in the hole effective mass parameters could lead to relatively large discrepancies in the binding energies. Our overall evaluation of parameters suggests that the better BE values are obtained with those in Ref. [25]. Correspondingly, we refer the reader to the first line in each impurity case in Tables V, VI, and VII, for what we consider the best BE estimates, within a few percent error. Further refinement of experimental values would be desirable to set narrower constraints on the theoret-

ical values. We also find that the binding energies for acceptors in the ZB structures are much shallower than their counterparts in the WZ structures, suggesting perhaps much more efficient carrier doping in those systems (yet to be observed experimentally).

Finally, we should mention that preliminary studies of the strain effects on the acceptor binding energies show an increase as the strain increases, although with a much stronger dependence than in other III-V materials. A complete report of these studies will be presented elsewhere.

ACKNOWLEDGMENTS

We thank K. Kim, W.R.L. Lambrecht and B. Segall for kindly communicating unpublished results to us, and for very helpful discussions. This work was supported in part by grants ONR-URISP N00014-96-1-0782, DURIP N00014-97-1-0315, and from CONACyT-México.

¹ S. Itoh *et al.*, Jpn. Appl. Phys. **32**, L1530 (1993); S. Nakamura *et al.*, *ibid.* **34**, L797 (1995); **34**, L1429 (1995); R.J. Molnar *et al.*, Appl. Phys. Lett. **66**, 268 (1995); S. Nakamura *et al.* *ibid.* **68**, 2105 (1996).

² R.L. Aggarwal *et al.*, J. Appl. Phys. **79**, 2148 (1996); S. Nakamura *et al.*, Jpn. J. Appl. Phys. **35**, L74 (1996).

³ B.W. Lim *et al.*, Appl. Phys. Lett. **68**, 3761 (1996).

⁴ S. Strite, H. Morkoç, J. Vac. Sci. Technol. B **10**, 1237, (1992); S. Strite, in *Properties of group III nitrides*, Chap. 9.5, 272-275, edited by J.H. Edgar (INSPEC, Kansas City, 1996), and references therein.

⁵ Z. Yang *et al.*, Appl. Phys. Lett. **67**, 1686 (1995); W. Götz *et al.* *ibid.* **68**, 667 (1996); W. Götz *et al.*, *ibid.* **68**, 3470 (1996); W. Kim *et al.* *ibid.*, Appl. **69**, 559 (1996).

⁶ S. Nakamura *et al.*, Jpn. J. Appl. Phys. **31**, 1258 (1992); M.S. Brandt *et al.*, Phys. Rev. B **49**, 14758 (1994).

⁷ S. Strite, Jpn. J. Appl. Phys. **33**, L699 (1994).

⁸ C.H. Park and D.J. Chadi, Phys. Rev. B **55**, 12995 (1997).

⁹ P. Boguslawski and J. Bernholc, Phys. Rev. B **56**, 9496 (1997); P. Boguslawski *et al.*, Appl. Phys. Lett. **69**, 233 (1996).

¹⁰ F. Bernardini *et al.*, Appl. Phys. Lett. **70**, 2990 (1997), and references therein.

¹¹ J. Neugebauer and C.G. Van de Walle, Appl. Phys. Lett. **68**, 1829 (1996).

¹² F. Fiorentini, F. Bernardini, A. Bosin, and D. Vanderbilt, in *Proceedings of the 23rd International Conference on the Physics of Semiconductors*, edited by M. Scheffler and R. Zimmerman (World Scientific, Singapore, 1996), p. 2877.

¹³ F. Bernardini, V. Fiorentini and R. M. Nieminen, in *Proceedings of the 23rd International Conference on the Physics of Semiconductors*, edited by M. Scheffler and R. Zimmerman (World Scientific, Singapore, 1996), p. 2881.

¹⁴ S.T. Pantelides, Rev. Mod. Phys. **50**, 797 (1978).

¹⁵ G.L. Bir and G.E. Pikus, *Symmetry and strain-induced effects in semiconductors* (Wiley, New York, 1974).

¹⁶ G.E. Pikus, Zh. Eksp. Teor. Fiz. **41**, 1258 (1961) [Sov. Phys. JETP **14**, 898 (1962)]; **41**, 1507 (1961)[**14**, 1075 (1962)].

¹⁷ J.M. Luttinger and W. Kohn, Phys. Rev. **97**, 869 (1955).

¹⁸ S. L. Chuang and C. S. Chang, Phys. Rev. B **54**, 2491 (1996).

¹⁹ J. Bernholc and S. T. Pantelides, Phys. Rev. B **15**, 4935 (1977).

²⁰ Y. M. Sirenko, J. B. Jeon, K. W. Kim, M. A. Littlejohn and M. A. Stroscio, Phys. Rev. **53**, 1997 (1996); Y. M. Sirenko *et al.* Phys. Rev. **55**, 4360 (1997).

²¹ P.K. Lam, M.L. Cohen and A. Zunger, Phys. Rev. B **22**, 1698 (1980).

²² A. Zunger and M.L. Cohen, Phys. Rev. B **18**, 5449 (1978).

²³ J. Sak, Phys. Rev. B **3**, 3356 (1971).

²⁴ X. Wu and F.M. Peeters, Phys. Rev. B **55**, 15438 (1997).

²⁵ K. Kim, W.R.L. Lambrecht, B. Segall, and M. van Schilfgaarde, Phys. Rev. B **56**, 7363 (1997).

²⁶ M. Suzuki, T. Uenoyama and A. Yanase, Phys. Rev. B **52**, 8132 (1995).

²⁷ J. A. Majewski, M. Städle, and P. Vogl, Mat. Res. Soc. Symp. Proc. **449**, 887 (1997).

²⁸ Y. C. Yeo, T. C. Chong and M. F. Li, to appear in Mat. Res. Soc. Symp. Proc. **482** (1998).

²⁹ R. Wang, P.P. Ruden, J. Kolnik, I. Oguzman and K.F. Brennan, Mat. Res. Soc. Symp. Proc. **449**, 935 (1997).

³⁰ A.T. Meney and E.P. O'Reilly, Appl. Phys. Lett. **67**, 3013 (1995).

³¹ A. Salvador, W. Kim, O. Aktas, A. Botchkarev, Z. Fan and H. Morkoc, Appl. Phys. Lett. **69**, 2692 (1996).

³² S. Fischer, C. Wetzel, E.E. Haller, and B.K. Meyer, Appl. Phys. Lett. **67**, 1298 (1995).

³³ N. V. Edwards, *et al.*, Appl. Phys. Lett. **70**, 2001 (1997).

³⁴ B. Gil, F. Hamdani, and H. Morkoç, Phys. Rev. B **54**, 7678 (1996).

³⁵ B. Gil, O. Briot, and R.L. Aulombard, Phys. Rev. B **52**, R17028 (1995).

³⁶ R. Dingle, D.D. Sell, S. E. Stokowski, and M. Illegems, Phys. Rev. B **4**, 1211 (1971).

³⁷ J. W. Lee, S. J. Pearton, J. C. Zolper, and R. A. Stall, Appl. Phys. Lett. **68**, 2102 (1996).

³⁸ I. Akasaki, H. Amano, M. Kito and K. Hiramoto, J. of Luminescence **48**, 666 (1991).

³⁹ D. J. As, F. Schmilgus, C. Wang, B. Schöttker, D. Schikora, and K. Lischka, Appl. Phys. Lett. **70**, 1311 (1997).

⁴⁰ O. Madelung, *Semiconductors-Basic Data*, (Springer, Marburg, 1996).

	C	Mg	Zn
Exp.	27.0	28.7	30.6
Theor.	27.4	27.7	28.3

TABLE I. Comparison between the experimental and the EMT-pseudopotential model of the acceptor binding energy for various impurities species in GaAs ($\epsilon_o = 12.4$). The energies are in meV. The experimental values and the band parameters are taken from Ref. [40].

WZ-GaN				
Ref.	[25]	[26]	[27]	[28]
A_1	-6.4	-6.27	-6.4	-7.24
A_2	-0.5	-0.96	-0.8	-0.51
A_3	5.9	5.70	5.93	6.73
A_4	-2.55	-2.84	-1.96	-3.36
A_5	-2.56	-3.18	-2.32	3.35
A_6	-3.06	-4.96	-3.02	-4.72
Δ_1	36	73	24	22
Δ_2	5.0	5.4	5.4	11/3
Δ_3	5.9	5.4	6.8	11/3
$\tilde{\gamma}_1$	2.91	3.80	2.76	3.87
E_o^*	51.8	39.7	54.6	39.0

TABLE II. The Rashba-Sheka-Pikus valence band parameters for wurtzite GaN. The hole parameters A_i are in units of $\hbar^2/2m_o$, while $\tilde{\gamma}_1$ is dimensionless; Δ_i values represent the energy splittings in meV; E_o^* is the effective Rydberg energy in meV. We use $\epsilon_o = 9.5$ as the dielectric constant in GaN. Signs of A_5 and A_6 parameters of Ref. [25] have been changed to be consistent with those in the definition of the usual RSP Hamiltonian.

WZ-AlN			
Ref.	[25]	[26]	[27]
A_1	-3.86	-4.06	-3.82
A_2	-0.25	-0.26	-0.22
A_3	3.58	3.78	3.54
A_4	-1.32	-1.86	-1.16
A_5	-1.47	-2.02	-1.33
A_6	-1.64	-3.04	1.25
Δ_1	-215	-58	-219
Δ_2	6.8	6.8	6.6
Δ_3	5.7	6.8	6.7
$\tilde{\gamma}_1$	1.57	2.12	1.38
E_o^*	119.9	88.8	136.5

TABLE III. The Rashba-Sheka-Pikus valence band parameters for wurtzite AlN. We use $\epsilon_o = 8.5$ as the dielectric constant in AlN. Parameters have the same units as indicated in Table II. Notice the enormous discrepancy in the crystal field splitting Δ_1 between Ref. [25], [27], and [26].

ZB-GaN			ZB-AlN		
Ref.	[25]	[26]	[29]	[25]	[26]
γ_1	2.46	2.70	2.94	1.40	1.50
γ_2	0.65	0.76	0.89	0.35	0.39
γ_3	0.98	1.07	1.25	0.59	0.62
Δ_o	19	20	17	19	20
E_o^*	51.3	55.8	49.3	134.5	125.5

TABLE IV. The Luttinger-Kohn valence band parameters for zincblende GaN and AlN. Here the dimensionless γ_i are the hole band parameters; Δ_o is the energy splitting due to spin-orbit interaction at the Γ point, and E_o^* are given in meV.

WZ-GaN			
Impurity <i>site</i>	E_b^*	E_b^{**}	E_b (Exp.)
Be _{Ga}	193	204	
	233	241	250 ^a
	195	208	
	185	193	
Mg _{Ga}	204	215	
	245	253	250 ^b
	208	221	
	197	204	
Zn _{Ga}	321	331	
	411	419	340 ^b
	394	406	
	352	360	
Ca _{Ga}	248	259	
	297	305	
	264	276	
	247	255	
C _N	220	230	
	264	272	230 ^c
	228	240	
	214	223	
Si _N	192	203	
	231	239	
	193	205	
	183	191	

^aReference [31]

^bReference [4]

^cReference [32]

TABLE V. Comparison between the calculated acceptor binding energies and experimental values for different substitutional impurities in wurtzite GaN. E_b^{**} and E_b^* denotes the estimated binding energies with and without the polaron correction. All energies are in meV. The binding energies are obtained with the band-parameters from Ref. [25], [26], [27], and [28], respectively, arranged in descending order for each impurity.

WZ-AlN		
Impurity <i>site</i>	E_b^*	E_b^{**}
Be _{Al}	223	262
	446	472
	283	253
Mg _{Al}	465	514
	758	795
	721	789
Zn _{Al}	219	255
	438	464
	273	343
Ca _{Al}	204	240
	376	402
	203	273
Si _N	214	250
	415	441
	245	315

TABLE VI. Calculated acceptor binding energies for different impurities in wurtzite AlN. Binding energies are ordered in descending order for parameters from Ref. [25], [26], and [27], respectively. The large discrepancy in the calculated values is mostly due to the important differences in the crystal field splitting used.

	ZB-GaN		ZB-AlN	
Impurity	E_b^*	E_b^{**}	E_b^*	E_b^{**}
Be	124	133	265	292
	117	125	248	273
	126	133		
Mg	130	139	333	360
	123	130	305	330
	133	140		
Zn	170	178	261	288
	155	162	245	269
	177	184		
Ca	153	162	242	268
	143	151	227	252
	157	164		
C	138	147	353	380
	130	138	320	345
	141	148		
Si	123	132	255	281
	117	125	239	264
	125	132		

TABLE VII. Acceptor states for zincblende GaN and AlN. The three values shown for impurities in GaN correspond to those calculated with the parameterizations given by Ref. [25], [26], and [29], respectively. The two values for AlN correspond to Ref. [25], and [26].

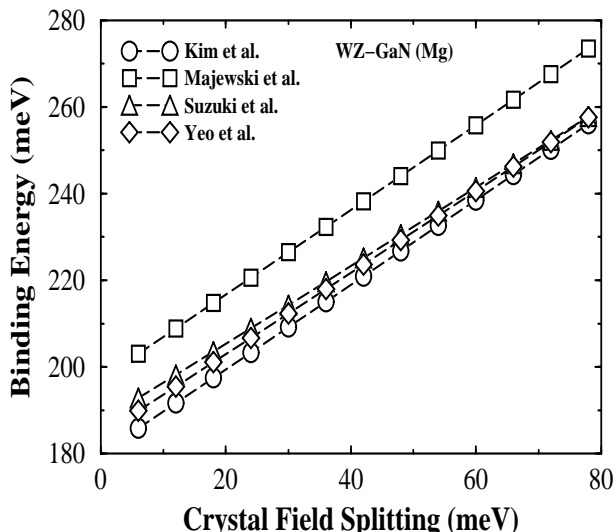


FIG. 1. Binding energies vs. crystal field splitting Δ_1 , in the Mg_{Ga} WZ-GaN system for different parameterizations. Different symbols correspond to binding energy values obtained from the effective mass parameters, \circ for Ref. [25], \triangle for Ref. [26], \square for Ref. [27], and \diamond for Ref. [28], respectively.